

# Altered modulation of WNT- $\beta$ -catenin and PI3K/Akt pathways in IgA nephropathy

Sharon N. Cox<sup>1,4</sup>, Fabio Sallustio<sup>1,4</sup>, Grazia Serino<sup>1</sup>, Paola Pontrelli<sup>2</sup>, Raffaella Verrienti<sup>1</sup>, Francesco Pesce<sup>1</sup>, Diletta D. Torres<sup>1</sup>, Nicola Ancona<sup>3</sup>, Patrizia Stifanelli<sup>3</sup>, Gianluigi Zaza<sup>1</sup> and Francesco P. Schena<sup>1</sup>

<sup>1</sup>Department of Emergency and Organ Transplantation, University of Bari, Bari, Italy; <sup>2</sup>Department of Biomedical Sciences, University of Foggia, Foggia, Italy and <sup>3</sup>ISSIA, CNR, Bari, Italy

Immunoglobulin A nephropathy (IgAN) is the most common form of primary glomerulonephritis worldwide. The basic defect lies within the IgA immune system and in peripheral blood leukocytes, rather than local kidney abnormalities. To define the intracellular mechanisms leading to the disease, we conducted a microarray study to identify genes and pathways differentially modulated in peripheral blood leukocytes isolated from 12 IgAN patients and 8 healthy controls. The genes whose expression discriminated between the IgAN patients and controls were primarily involved in canonical WNT- $\beta$ -catenin and PI3K/Akt pathways. We also tested peripheral blood mononuclear cells and their subpopulations isolated from an independent group of IgAN patients and healthy controls. There were low protein levels of inversin and PTEN, key regulators of WNT- $\beta$ -catenin and PI3K/Akt, in IgAN patients, suggesting hyperactivation of these pathways. Also, there were increased phospho-Akt protein levels and nuclear  $\beta$ -catenin accumulation with an enhanced peripheral blood mononuclear cell proliferation rate. Subpopulation analysis uncovered a major irregularity of WNT signaling in monocytes. Hence, hyperactivation of these pathways may provide insight into mechanisms contributing to the pathogenesis of IgAN.

*Kidney International* (2010) **78**, 396–407; doi:10.1038/ki.2010.138; published online 19 May 2010

KEYWORDS: gene expression; IgA nephropathy; lymphocytes; proliferation; signaling

**Correspondence:** Francesco P. Schena, Nephrology Dialysis and Transplantation Unit, Department of Emergency and Organ Transplantation, University of Bari, Policlinico, Piazza G. Cesare no 11, 70124 Bari, Italy.  
E-mail: fp.schena@nephro.uniba.it

<sup>4</sup>These two authors contributed equally to this work.

Received 31 July 2009; revised 24 February 2010; accepted 16 March 2010; published online 19 May 2010

Immunoglobulin A (IgA) nephropathy (IgAN) is the most common form of primary glomerulonephritis worldwide among patients undergoing renal biopsy. The diagnosis is based on the occurrence of mesangial IgA deposits in the glomeruli and the presence of recurrent episodes of intrarenal macroscopic hematuria, or persistent microscopic hematuria, and/or proteinuria.<sup>1,2</sup> IgAN is characterized by dysregulation of the immune system, leading to an abnormal deglycosylated IgA1 synthesis, selective mesangial IgA1 deposition with ensuing mesangial cell proliferation, and extracellular matrix expansion, through poorly understood molecular mechanisms.<sup>3,4</sup> Approximately 40% of IgAN patients, older than 30 years, develop end-stage renal disease within 20 years of disease onset.<sup>5</sup>

Recurrence of IgA deposits in IgAN patients after transplantation indicates that the basic abnormality of this condition lies within the IgA immune system, rather than local kidney abnormalities.<sup>6–8</sup> This is further strengthened by the observation that IgA deposits disappear when a graft containing mesangial IgA deposits is accidentally transplanted in recipients not suffering from IgAN.<sup>9</sup>

Human IgA production occurs in two distinct immunological compartments: mucosa and bone marrow; IgA produced at mucosal surfaces is almost exclusively polymeric (pIgA). Serum IgA, which is mostly monomeric, arises from the systemic immune compartment and is mainly produced in the bone marrow. Immunization studies on IgAN patients show elevated systemic pIgA secretion in response to both systemic and mucosal antigens.<sup>10–12</sup> Therefore, although the circulating pIgA in IgAN arises from a systemic source, it may be driven by mucosally encountered antigens, such as bacteria and viruses.<sup>11,12</sup> This scenario strongly suggests that an abnormal control of the fine balance between the mucosal and systemic immune systems may contribute to the pathogenesis of IgAN.<sup>13,14</sup> Hyperresponsiveness of the IgA immune system in IgAN patients is confirmed by increased IgA-secreting plasma cell number in both bone marrow and tonsils.<sup>15–17</sup> These cells show a reduced susceptibility to Fas-mediated apoptosis with marked expression of bcl-2.<sup>17</sup>

Several research strategies have been used to study the pathogenesis of this complex disease; however, few have provided specific descriptions of the intracellular

mechanisms associated with disease development.<sup>18</sup> As peripheral blood leukocytes (PBLs) of IgAN patients carry informative disease-specific markers,<sup>19</sup> their gene expression profile was used in our study to screen for new pathways and mechanisms differently regulated in the disease. We specifically found an aberrant modulation of WNT-β-catenin and PI3K/Akt pathways. Further, we observed that these pathways were hyperactivated in peripheral blood mononuclear cells (PBMCs) of an independent group of IgAN patients. These cells were characterized by an increased Akt phosphorylation, β-catenin nuclear translocation, and proliferation rate. These results could contribute to shed light into the key pathogenetic mechanisms of IgAN.

## RESULTS

### Differences in gene expression between IgAN patients and healthy subjects

To uncover new molecular mechanisms involved in IgAN pathogenesis, we compared the genomic profile of PBLs in a group of 12 IgAN patients and 8 healthy subjects (HS) with normal renal function, after having their informed consent. Bioinformatic analysis revealed 210 genes discriminating IgAN patients from HS (false discovery rate (FDR)-adjusted  $P$ -value < 0.01) (Supplementary Tables S1, S2). The two-dimensional hierarchical clustering, using the 210 genes, clearly showed the degree of separation between IgAN patients and HS (Figure 1). Ingenuity pathway analysis (IPA) showed that the identified genes were primarily involved in WNT-β-catenin and PI3K/Akt canonical pathways (FDR-adjusted  $P = 0.0039$  and  $P = 0.004$ , respectively) (Table 1). In addition, the top ranked network included several genes encoding for regulators of these pathways, for example, inversin (*INV*)<sup>20</sup> (Figure 2).

We then moved on to investigate whether the identified set of genes were also able to separate IgAN from other glomerular diseases. We compared the previously identified set of genes, discriminating IgAN patients from HS, with the gene expression profile of PBLs from three focal segmental glomerulosclerosis patients and from three membranoproliferative glomerulonephritis type I patients. Gene set enrichment analysis<sup>21</sup> (GSEA) identified subsets of 22 and 19 genes specific for membranoproliferative glomerulonephritis type I and focal segmental glomerulosclerosis, respectively, and a subset of 21 genes able to specifically separate IgAN from HS and from both glomerular diseases (FDR-adjusted  $P$ -value < 0.05) (Supplementary Figure S1). This subset of genes, specific for IgAN, was again primarily involved in WNT-β-catenin and PI3K/Akt canonical pathways (data not shown).

### Figure 1 | 2-Dimensional hierarchical clustering using the top 210 selected genes discriminating 12 immunoglobulin A nephropathy (IgAN) patients from 8 healthy subjects (HS).

Each column represents a subject and each row a gene probe set. Probe set signal values were normalized to the mean across the patients. The relative level of gene expression is depicted from the lowest (green) to the highest (red), according to the scale shown on the top. Respective gene symbols are indicated on the right side.

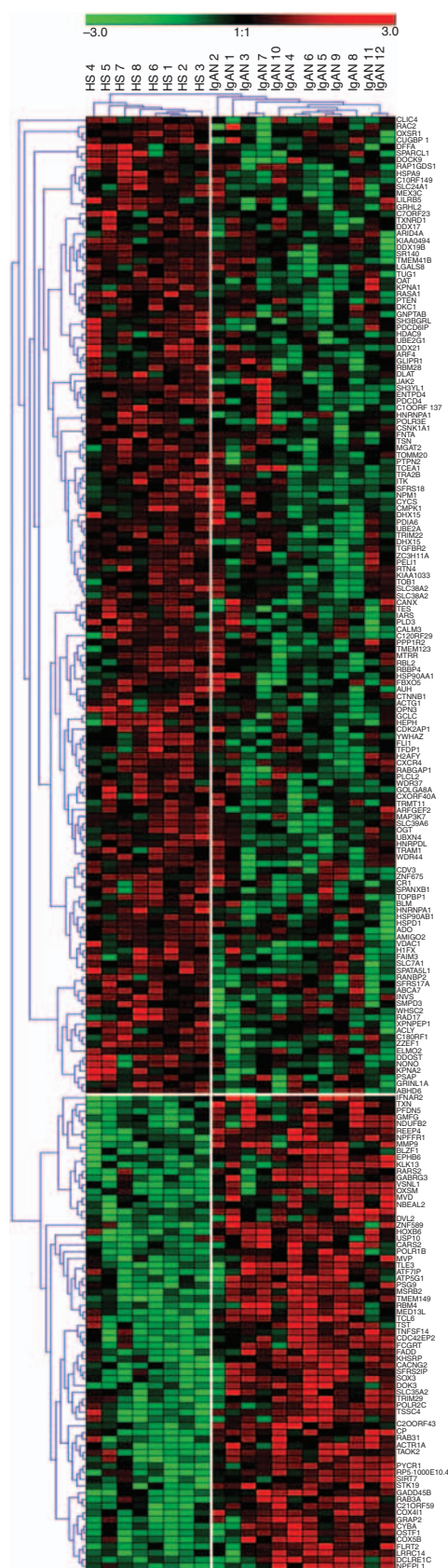


**Table 1 | Most representative canonical pathways deregulated in IgAN patients**

IPA category	Pathway P-value <sup>a</sup>	Gene symbol	Gene name	Probe set ID
PI3K/Akt signaling	0.0040	<i>CSNK1A1</i>	Casein kinase 1, α1	208867_s_at
		<i>CTNNB1</i>	Catenin β1 (88 kDa)	201533_at
		<i>HSP90AB1</i>	Heat shock protein-α (90 kDa) class B member 1	200064_at
		<i>HSP90AA1</i>	Heat shock protein (90 kDa) class A member 1	210211_s_at
		<i>PTEN</i>	Phosphatase and tensin homolog	204054_at
		<i>JAK2</i>	Janus kinase 2	205842_s_at
		<i>YWHAZ</i>	Tyrosine 3-monooxygenase/tryptophan 5-monooxygenase activation protein, ζ-polypeptide	200641_s_at
WNT-β-catenin signaling	0.0039	<i>CSNK1A1</i>	Casein kinase 1, α1	208867_s_at
		<i>INV</i>	Inversin	211055_s_at
		<i>CTNNB1</i>	Catenin β1 (88 kDa)	201533_at
		<i>SOX3</i>	SRY (sex determining region Y)-box 3	214633_at
		<i>TGFBR2</i>	Transforming growth factor, β-receptor II	208944_at
		<i>TLE3</i>	Transducin-like enhancer of split 3 (E (sp1) homolog, Drosophila)	212770_at
		<i>DVL2</i>	Dishevelled, dsh homolog 2 (Drosophila)	57532_at
		<i>MAP3K7</i>	Mitogen-activated protein kinase kinase kinase 7	211537_x_at

Abbreviations: FDR, false discovery rate; IgAN, immunoglobulin A nephropathy; IPA, ingenuity pathway analysis.  
<sup>a</sup>Fischer's exact test was used to calculate the P-value, determining the probability that the association between the genes in the data set and the canonical pathway is explained by chance alone. To account for multiple canonical pathways tested by IPA, the FDR option was used (FDR < 0.1).

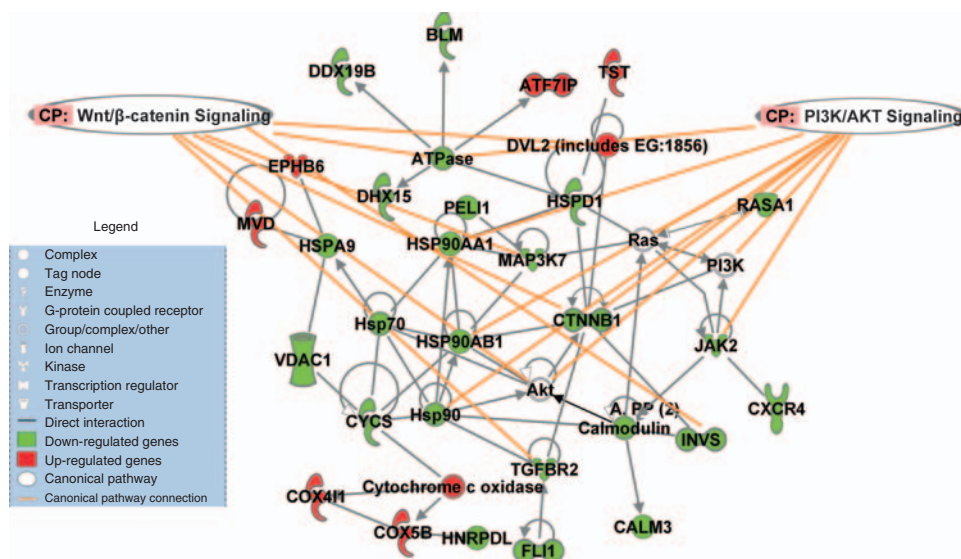


**Figure 2 | Functional analysis of the top selected genes identified by microarray.** The network was algorithmically constructed by Ingenuity Pathway Analysis (IPA) software on the basis of the functional and biological connectivity of genes. The network is graphically represented as nodes (genes) and edges (the biological relationship between genes). Red and green shaded nodes represent up- and downregulated genes, respectively; others (empty nodes) are those that IPA automatically includes because they are biologically linked to our genes based on the evidence in the literature. This top ranked network (score 48,  $n = 27$  associated genes,  $P < 0.0001$ , Figure 2) includes several genes encoding for regulators of the PI3K/Akt pathway (β-catenin (*CTNNB1*), heat shock protein 90 kDa (*HSP90AB1*), heat shock protein 90 kDa alpha, class A member 1 (*HSP90AA1*) janus kinase 2 (*JAK2*)) and molecular switches of the WNT-β-catenin pathway (inversin (*INV*) and dishevelled, homolog 2 (*DVL2*)). Meanings of node shapes and edges are indicated in the legend within the figure.

To further establish the validity of gene expression determined by microarray analysis, we performed quantitative real-time PCR (RT-PCR) on all patient and HS samples that were used for the microarray study. We chose two key regulators of WNT-β-catenin and PI3K/Akt pathways, *INV* and phosphatase and tensin homolog (*PTEN*); mRNA levels for these genes were found significantly lower in IgAN group compared with HS subjects ( $P = 0.02$ ,  $P = 0.003$ , respectively) (Figure 3a and b). Furthermore, Pearson's correlation

coefficient between mRNA levels determined by RT-PCR and microarray was 0.78 for *INV* ( $P < 0.001$ ) and 0.74 for *PTEN* ( $P < 0.002$ ), confirming expression levels determined by the gene expression array (Figure 3c and d).

**INV and PTEN protein levels in IgAN patients**

Moving from the modulation of WNT-β-catenin and PI3K/Akt pathways emerging from gene expression analysis in PBLs, we then investigated whether the same abnormality

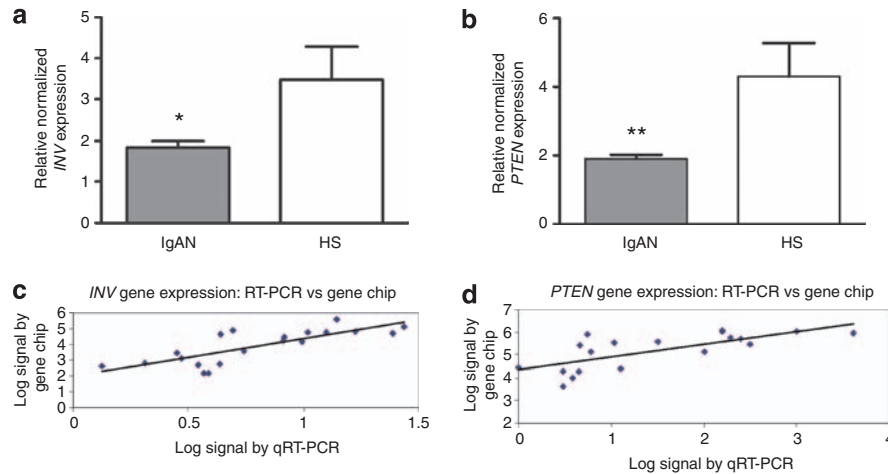


**Figure 3 | *Inversin (INV)* and *phosphatase and tensin homolog (PTEN)* gene expression levels evaluated by reverse transcriptase PCR (RT-PCR) directly correlate with microarray expression data in 12 immunoglobulin A nephropathy (IgAN) patients and 8 healthy subjects (HS).** The histograms represent the mean  $\pm$  s.e.m. of the relative normalized protein expression of each protein evaluated by RT-PCR; *INV* (a) and *PTEN* (b) protein levels are significantly lower in 12 IgAN patients compared with 8 HS (\* $P=0.019$ , \*\* $P=0.003$ , respectively). The mRNA levels for the gene *INV* (c) and *PTEN* (d) determined by quantitative RT-PCR (qRT-PCR) correlate with microarray expression scores (Pearson's  $r$  for *INV* = 0.78;  $P=0.0001$  and *PTEN* = 0.74;  $P=0.0002$ ; data are shown as  $\log_2$ ).

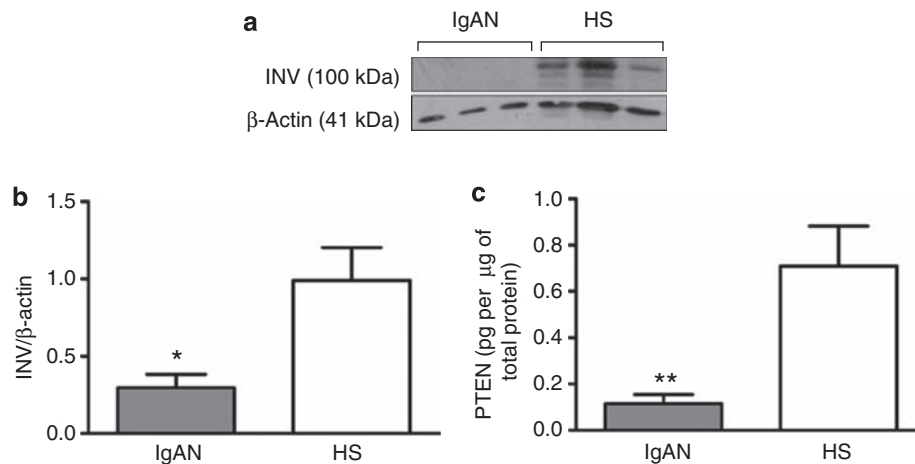


**Figure 4 | *Inversin (INV)* and *phosphatase and tensin homolog (PTEN)* protein expression levels in peripheral blood mononuclear cells (PBMCs) from immunoglobulin A nephropathy (IgAN) patients and healthy subjects (HS).** (a) Representative western blotting experiment for *INV*. (b) *INV* protein levels of nine IgAN patients and eight HS assessed by western blotting. In accordance with mRNA expression levels, *INV* protein levels are significantly lower in IgAN patients compared with HS (\* $P=0.006$ ). (c) *PTEN* protein levels of seven IgAN patients and seven HS assessed by enzyme-linked immunosorbent assay (ELISA), the protein levels are significantly lower in IgAN compared with HS (\*\* $P=0.007$ ). The histograms represent the mean  $\pm$  s.e.m. of *INV* and *PTEN* protein levels.

occurred in PBMCs, a population that is known to be principally involved in IgAN pathogenesis.<sup>22–24</sup> We measured the protein levels of *INV* and *PTEN* in PBMC lysate of IgAN patients and HS. The *INV* levels were significantly lower in IgAN patients ( $0.29 \pm 0.08$  *INV*/ $\beta$ -actin ratio) compared with HS ( $0.99 \pm 0.2$  *INV*/ $\beta$ -actin ratio,  $P=0.006$ ) (Figure 4a and b). *PTEN* was significantly lower in IgAN patients ( $0.1150 \pm 0.03914$  pg/ $\mu$ g of total protein) compared with HS ( $0.7100 \pm 0.1720$  pg/ $\mu$ g of total protein,  $P=0.007$ ) (Figure 4c).

#### Intracellular activation of Akt in IgAN patients

To evaluate whether low *PTEN* expression was associated with activation of the PI3K/Akt pathway,<sup>25,26</sup> we measured

the level of Akt protein phosphorylation in PBMCs of IgAN patients. We found phosphorylated Akt (p-Akt) to total Akt ratios significantly higher in IgAN patients ( $7.372 \pm 1.965$  p-Akt (pg/ml)/total Akt (ng/ml)) compared with HS ( $2.510 \pm 0.7530$  p-Akt (pg/ml)/total Akt (ng/ml);  $P=0.04$ ) (Figure 5a). This result was not due to a difference in total Akt between IgAN patients and HS (Supplementary Figure S2).

#### Nuclear $\beta$ -catenin accumulation in IgAN patients

To assess whether hyperactivation of Akt and the down-regulation of *INV* may induce nuclear  $\beta$ -catenin accumulation<sup>20,27</sup> in IgAN patients, we measured the level of nuclear translocation of this protein in PBMCs isolated from both

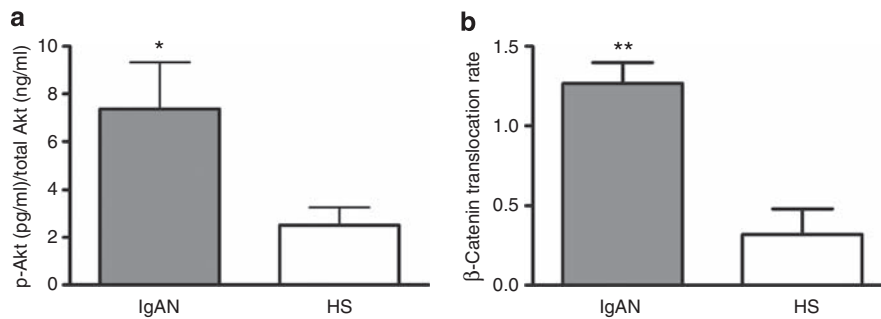


**Figure 5 | Activation of Akt and  $\beta$ -catenin nuclear accumulation in peripheral blood mononuclear cells (PBMCs) from immunoglobulin A nephropathy (IgAN) patients and healthy subjects (HS).** (a) Activation of Akt in seven IgAN patients and seven HS, as measured by enzyme-linked immunosorbent assay (ELISA). The histograms illustrate the ratio of phosphorylated Ser473 Akt to total Akt, expressed as a mean  $\pm$  s.e.m. The ratios were significantly higher in IgAN patients compared with HS ( $*P = 0.04$ ). (b) Nuclear and cytoplasmic extracts from PBMCs of seven IgAN patients and seven HS were prepared and assayed for  $\beta$ -catenin protein expression. A significantly higher translocation index was found in the IgAN patient group ( $1.2 \pm 0.13$ ) compared with HS ( $0.32 \pm 0.16$ ;  $**P = 0.0007$ ). The histograms represent the mean  $\pm$  s.e.m. of the  $\beta$ -catenin translocation index, expressed as a ratio of normalized nuclear  $\beta$ -catenin content over normalized cytoplasmic  $\beta$ -catenin content.

IgAN patients and HS. The  $\beta$ -catenin translocation index, expressed as the ratio of normalized nuclear  $\beta$ -catenin and normalized cytoplasmic  $\beta$ -catenin content, was significantly higher in IgAN patients ( $1.2 \pm 0.13$ ) compared with HS ( $0.32 \pm 0.16$ ;  $P = 0.0007$ ) (Figure 5b).

#### PBMC proliferation assay in IgAN patients

According to the results given above, hyperactivation of both WNT- $\beta$ -catenin and PI3K/Akt pathways was shown in IgAN patients. As these pathways are involved in the cellular machinery that regulate cell proliferation,<sup>28,29</sup> we studied PBMC proliferation, after mitogenic stimulation with concanavalin A, in IgAN patients compared with HS. The PBMC proliferation index was  $2.58 \pm 0.087$ -fold greater in IgAN patients compared with HS ( $P = 0.004$ ) (Figure 6a and b). In addition, in all subjects, the PBMC proliferation index was positively correlated with the ratio of p-Akt to total Akt (Pearson's  $r = 0.8443$ ;  $P = 0.0001$ ) (Figure 6c). An enhanced proliferation rate was also found when we stimulated PBMCs of IgAN patients with *Staphylococcus aureus* Cowan ( $P = 0.003$ ) and pokeweed mitogen ( $P = 0.04$ ) (Figure 6d and e).

#### WNT signaling pathways in PBMC subpopulations

Our next aim was to investigate which PBMC subpopulation maybe principally involved in the WNT signaling alteration seen in IgAN patients. We isolated T-lymphocytes (CD3+), B-lymphocytes (CD19+), and monocytes (CD14+) from PBMCs and used a WNT pathway PCR Array (SABiosciences Corporation, Frederick, MD, USA) to compare the transcript levels of 84 pathway genes in IgAN patients and HS. We found a different number and distribution of the modulated genes in IgAN patients in the three PBMC subsets (Figure 7a-d). Monocytes isolated from IgAN patients showed an hyperactivation of the WNT pathway compared with HS; in particular, we found 25 significantly regulated genes, 24 of which were upregulated (fold change  $> 1.5$  and  $P < 0.05$ ) (Supplementary Table S3). These identified genes generated a top ranked network in IPA (Figure 7e), centered around the

PI3K/Akt pathway. B-lymphocytes in IgAN patients showed a more blunt modulation, as nine genes were found to be significantly regulated, eight of them overlapping with altered monocyte genes (Supplementary Table S4). The WNT pathway was not significantly altered in T-lymphocytes, as only five genes were found deregulated in IgAN patients (Supplementary Table S5).

#### INV and PTEN protein levels in PBMC subpopulations from IgAN patients

Next, we measured the protein levels of INV and PTEN in PBMC subpopulations of IgAN patients and HS. The INV and PTEN levels were significantly lower in monocytes, B- and T-lymphocytes isolated from IgAN patients compared with HS ( $P < 0.04$  for all samples) (Figure 8a-c).

#### DISCUSSION

Several reports have investigated the molecular mechanisms underlying the complex pathogenesis of IgAN.<sup>18,30</sup> However, to date, only a single report applied high-throughput technologies to identify genes differently regulated in IgAN patients compared with HS, but the multifactorial interactions and complex biological networks among these genes were not examined.<sup>19</sup> On the contrary, in this study, a whole-genome expression analysis was used to uncover new mechanisms involved with the onset of IgAN. We selected a group of IgAN patients characterized by normal renal function. This rationale was used to identify genes associated with disease onset and not with disease progression. In fact, the inflammatory phenotype associated with the deterioration of the renal function could alter the gene expression profile, masking the genes that effectively contribute to the disease onset. In PBLs, we found several genes that were able to discriminate IgAN patients from HS; these genes generated highly significant networks and canonical pathways principally involving WNT- $\beta$ -catenin and PI3K/Akt pathways. The specificity of these pathways in IgAN patients compared with other types of glomerulonephritis was confirmed with GSEA.

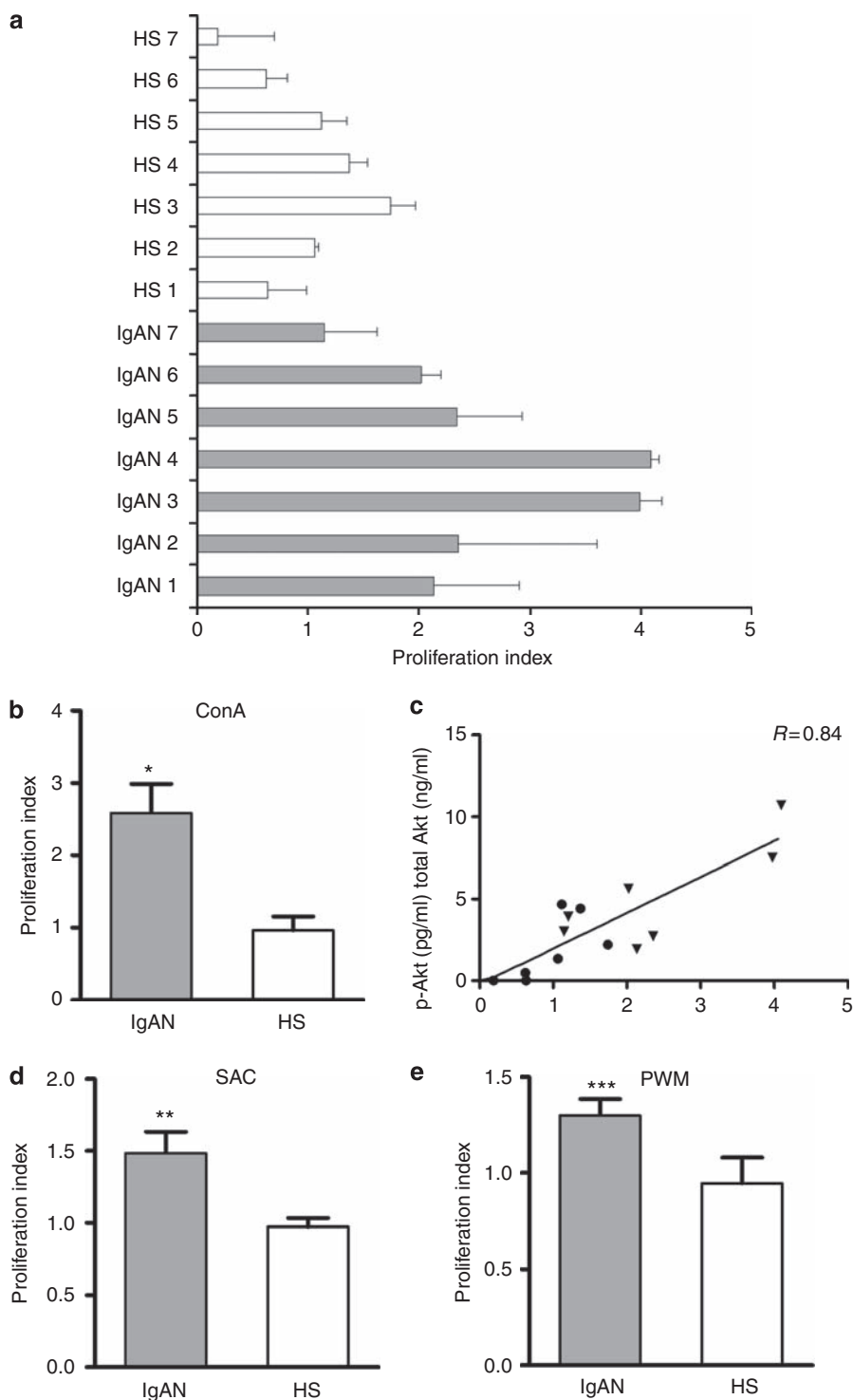


**Figure 6 | *In vitro* proliferation of peripheral blood mononuclear cells (PBMCs) isolated from immunoglobulin A nephropathy (IgAN) patients compared with healthy subjects (HS) in response to mitogenic stimulation. (a)** The proliferation index for each subject was calculated as the ratio between the 5-bromo-2-deoxyuridine (BrdU) absorbance in the test wells (containing PBMCs stimulated with concanavalin A (ConA)) and that in the control wells (containing unstimulated PBMCs). Results are representative of four independent experiments. **(b)** Cumulative results of all four experiments. PBMCs from seven IgAN patients show an increased proliferation rate compared with seven HS after mitogenic stimulation with ConA (5  $\mu$ g/ml). **(c)** The plot shows a direct correlation between the ratio of phosphorylated Akt to total Akt and the proliferation index (Pearson's  $r = 0.84$  and  $P = 0.0001$ , respectively,  $\blacktriangledown$  = IgAN,  $\bullet$  = HS). **(d)** PBMCs from seven IgAN patients show an increased proliferation rate compared with seven HS after mitogenic stimulation with *Staphylococcus aureus* Cowan (0.075% (wt/vol)). **(e)** PBMCs from seven IgAN patients show an increased proliferation rate compared with seven HS after mitogenic stimulation with pokeweed mitogen (10  $\mu$ g/ml). The histograms represent the mean  $\pm$  s.e.m. \* $P = 0.004$ ; \*\* $P = 0.003$ ; \*\*\* $P = 0.04$ .

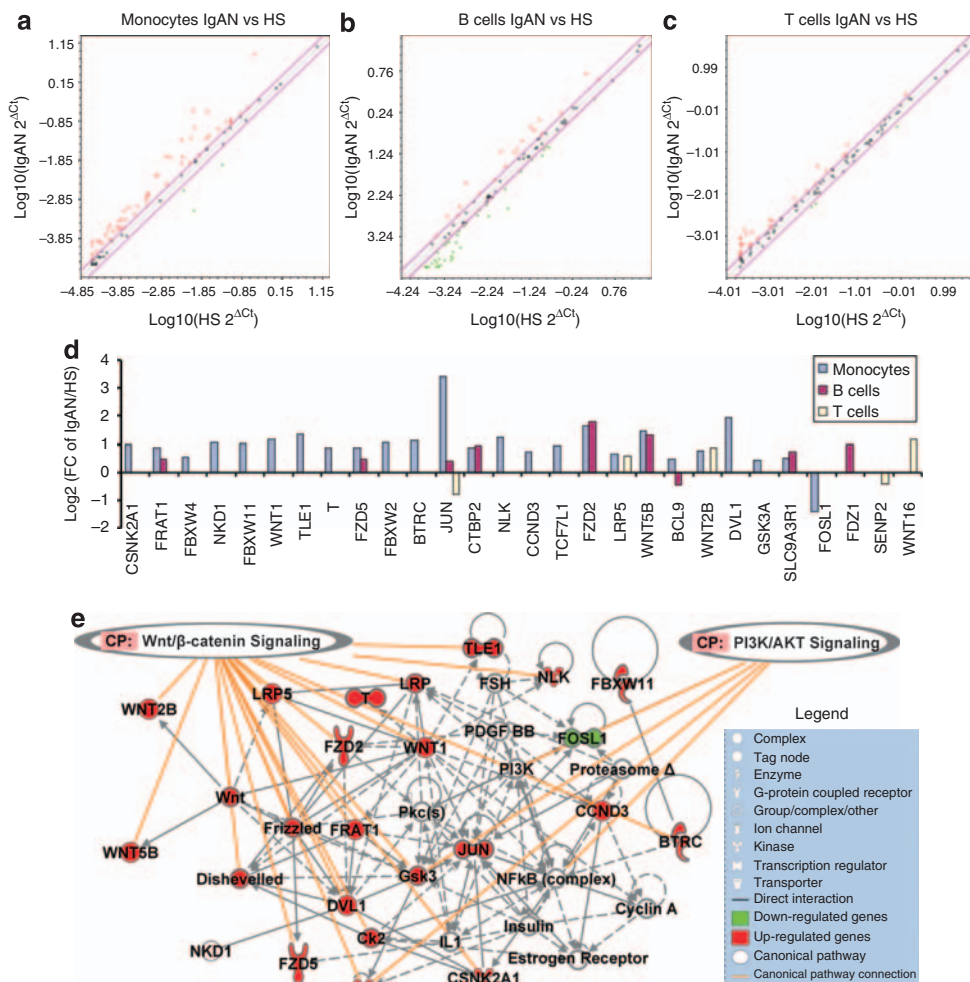


**Figure 7 | WNT gene array changes in peripheral blood mononuclear cell (PBMC) subpopulations from immunoglobulin A nephropathy (IgAN) patients.** (a–c) The scatter plots show the log transformation of the relative expression level of each gene ( $2^{-\Delta Ct}$ ) between IgAN and HS in monocytes, B- and T-lymphocytes. The pink lines indicate the 1.5-fold change in gene expression threshold. Red and green shaded dots indicate up- and downregulated genes, respectively. (d) Statistically relevant genes modulated in PBMC subpopulations isolated from IgAN patients compared with HS (fold difference > 1.5 and  $P < 0.05$ ). Most genes are altered in monocytes, eight of them overlap with the altered B-lymphocyte genes. The WNT pathway seems less altered in T-lymphocytes, as only five genes are deregulated in IgAN patients. (e) Top ranked network generated by IPA with monocyte modulated genes (score 52,  $n = 16$  associated genes;  $P < 0.0001$ ). This network is centered around the canonical pathway PI3K/Akt.

Our next aim was to discover whether these pathways were also aberrantly modulated in PBMCs isolated from an independent group of 16 IgAN patients and 16 HS, as PBMCs are known to be principally involved in IgAN pathogenesis.<sup>22–24</sup> We specifically found (a) lower INV and PTEN protein levels; (b) increased Akt protein phosphorylation; (c) augmented β-catenin translocation rate; and (d) enhanced *in vitro* proliferation rate after mitogenic stimulation (Figure 9). Abnormal WNT signaling was further confirmed in IgAN patients’ monocytes and to a lesser extent in B-lymphocytes.

The hyperactivation of the PI3K/Akt pathway was shown by low PTEN levels and by Akt protein activation in PBMCs of IgAN patients compared with HS. As previously described in human and animal models, the perturbation of the PI3k/Akt pathway seems to overlap the phenotypical features of IgAN.<sup>31–33</sup> In line with our results, a recent report on the study conducted on PBMCs of IgAN patients shows that

nuclear factor-κB, the downstream effector of activated Akt, has a greater translocation rate.<sup>24</sup>

Interestingly, PBMCs isolated from IgAN patients showed a higher proliferation rate compared with the control. The hyperactivation of these newly identified pathways in IgAN patients may be responsible for this enhanced proliferation, and may explain the increased cell number in both bone marrow and tonsils and the reduced susceptibility to Fas-mediated apoptosis in IgAN patients.<sup>15–17</sup> In particular, the hyperactivation of WNT signaling in B-lymphocytes from IgAN patients was confirmed with the PCR array. This pathway is known to regulate B-lymphocyte proliferation through lymphoid enhancer factor 1 (*LEF-1*).<sup>34</sup> Surprisingly, *LEF-1* is located within the region that we observed to be linked with IgAN on chromosome 4q26–31.<sup>35</sup>

In WNT signaling, WNT molecules bind to members of the Frizzled receptor protein family to activate dishevelled

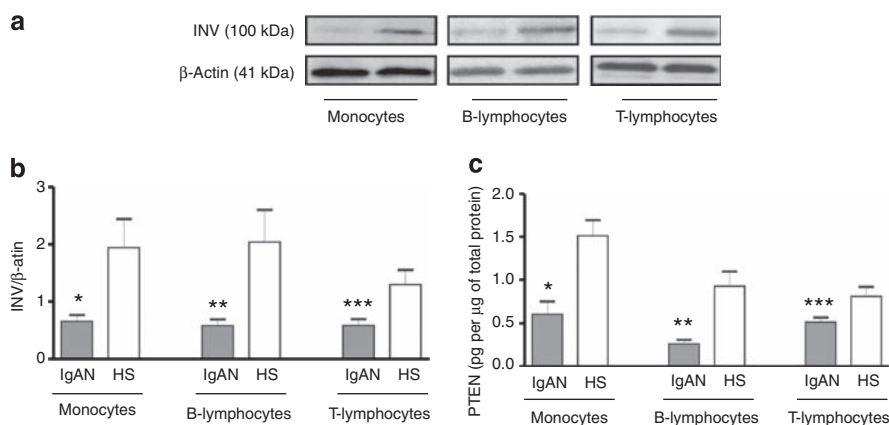


**Figure 8 | Inversin (INV) and phosphatase and tensin homolog (PTEN) protein expression levels in peripheral blood mononuclear cell (PBMC) subpopulations from immunoglobulin A nephropathy (IgAN) patients and healthy subjects (HS).** (a) Representative western blotting experiment for INV in PBMC subpopulations from IgAN patients and HS. (b) INV protein levels of six IgAN patients and six HS assessed by western blotting. In accordance with PBMCs protein levels, INV protein levels are significantly lower in monocytes, B- and T-lymphocytes from IgAN patients compared with HS ( $*P = 0.036$ ,  $**P = 0.027$ ,  $***P = 0.029$ ). (c) PTEN protein levels of six IgAN patients and six HS assessed by enzyme-linked immunosorbent assay (ELISA). The protein levels are significantly lower in monocytes, B- and T-lymphocytes from IgAN patients compared with HS ( $*P = 0.005$ ,  $**P = 0.004$ ,  $***P = 0.04$ ). The histograms represent the mean  $\pm$  s.e.m. of INV and PTEN protein levels.

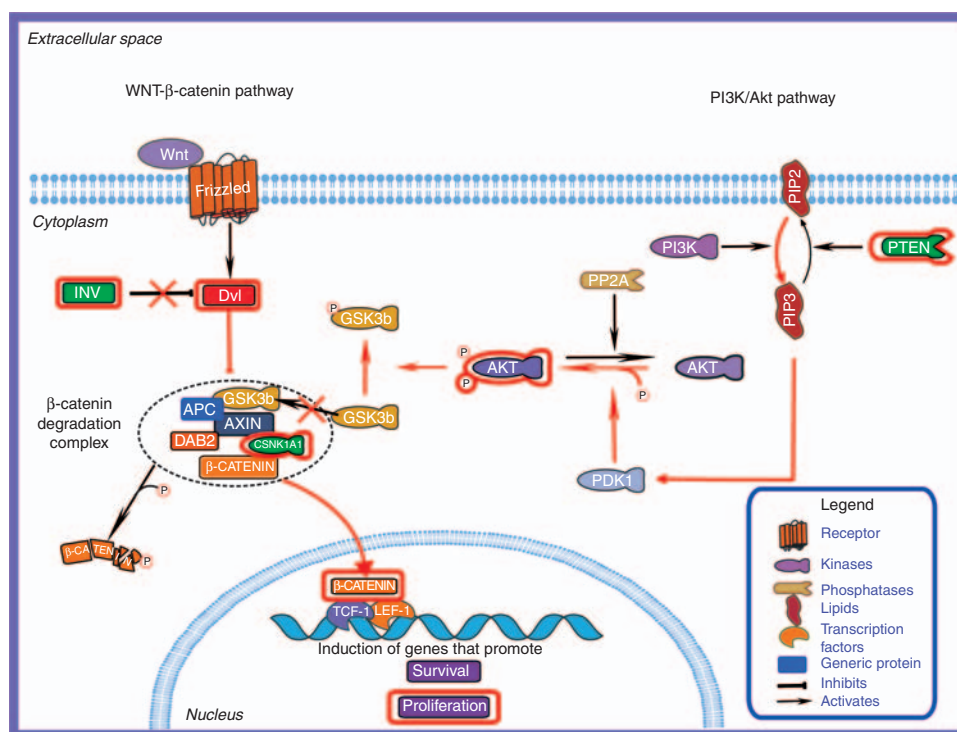


**Figure 9 | Hyperactivation of WNT-β-catenin and PI3K/Akt pathways in IgAN patients.** Altered modulation of WNT-β-catenin and PI3K/Akt pathways was shown at both the transcriptional and protein level in IgAN patients compared with healthy subjects. Specifically, we observed: (1) a downregulation of a gene encoding CSNK1A1, an active constituent of the β-catenin degradation complex; (2) an upregulation of DVL2, an intracellular β-catenin stabilizer; (3) lower inversin (INV) and phosphatase and tensin homolog (PTEN) protein levels; (4) hyperactivation of Akt by phosphorylation; and (5) an augmented β-catenin translocation rate. The altered modulation of WNT-β-catenin and PI3K/Akt pathway components contributes to the constitutive hyperactivation of these pathways, explaining the observed enhanced proliferation of peripheral blood mononuclear cells (PBMCs) in IgAN patients. The red circled symbols indicate pathway components studied in this work; red arrows indicate the pathway direction based on gene and protein expression data. The green and red shaded symbols indicate, respectively, down- and upregulated components found within the pathways.

(Dvl).<sup>36,37</sup> This activation inhibits β-catenin degradation, which translocates to the nucleus triggering transcriptional responses involved in cell survival, proliferation, and

differentiation.<sup>34,38,39</sup> Among the WNT-β-catenin genes identified by genomic analysis, *INV* reached a high level of significance. *INV* protein targets Dvl for degradation, leading

to reduced stabilized cytoplasmic  $\beta$ -catenin and WNT signaling.<sup>20</sup> Therefore, INV, downregulated at both mRNA and protein levels in our IgAN patients, represents the abnormal key regulator of this pathway, suggesting hyperactivation of WNT- $\beta$ -catenin signaling. A further dissection of this aberrancy was carried out with PCR array gene profiling on PBMC subpopulations, wherein we observed abnormal WNT signaling in IgAN patients' monocytes and, to a lesser extent, in B-lymphocytes. Recent studies highlight the emerging role of WNT pathway in orchestrating adaptive immunity in response to microbial stimulation of innate immune cells.<sup>40-43</sup> An hyperactivation of this pathway in monocytes and B-lymphocytes could lead to a defect in antigen handling and to abnormal systemic responses to mucosally encountered antigens, as seen in IgAN patients.<sup>10-12</sup> Monocytes, in particular, could have a pathogenic role in IgAN, as pIgA aggregates the Fc $\alpha$ RI on monocytes in IgAN patients and induces shedding of the extracellular domain to form circulating IgA1-Fc $\alpha$ RI complexes.<sup>44-46</sup> Furthermore, this receptor is activated through PI3K,<sup>47</sup> which seems to have a central role in IgAN patients' monocytes.

In conclusion, the altered modulation of the WNT- $\beta$ -catenin and PI3K/Akt pathways in our IgAN patients may provide new explanations for the mechanisms underlying some but not all the features of the immunopathogenesis of the disease. Further studies will be needed to better define the role of hyperactivation of WNT- $\beta$ -catenin and PI3K/Akt signal transduction pathways in IgAN. Finally, these mechanisms could be exploited for the identification of specific targets for the treatment of the disease.

## MATERIALS AND METHODS

### Sample donors

A total of 38 biopsy-proven IgAN patients and 34 HS were included in this study (Table 2). All patients and HS provided their informed consent. IgAN patients were characterized by normal renal function, whereas patients with moderate and severe renal damage were excluded from the study. In addition, subjects suffering from diabetes, chronic lung disease, cardiovascular diseases, neoplasm, or inflammatory diseases, and IgAN patients with renal transplantation receiving corticosteroids and immunosuppressive agents were

**Table 2 | Demographic and clinical features of IgAN patients and healthy subjects included in the study<sup>a</sup>**

	IgAN	HS
Number	38	34
Male/female	28/10	24/10
Age (years)	41.1 $\pm$ 6.9	39.3 $\pm$ 9.1
sCr (mg/dl)	0.9 $\pm$ 0.2	0.8 $\pm$ 0.3
eGFR	110.5 $\pm$ 10.7	106 $\pm$ 13.1
Proteinuria (24 h; g/l)	0.2 $\pm$ 0.02	0.1 $\pm$ 0.02
Systolic BP (mm Hg)	115.3 $\pm$ 7.8	120 $\pm$ 0.5
Diastolic BP (mm Hg)	75.5 $\pm$ 8.1	76 $\pm$ 4.1

Abbreviations: eGFR, estimated glomerular filtration rate calculated with the Cockcroft-Gault formula (ml/min per 1.73 m<sup>2</sup>); IgAN, immunoglobulin A nephropathy patients; HS, healthy subjects; sCr, serum creatinine.

<sup>a</sup>Values are expressed as mean  $\pm$  s.d.

excluded from the study. Furthermore, patients suffering from a viral or bacterial upper respiratory tract infection were also excluded beforehand. IgAN patients were collected regardless of their having a familial or sporadic form of the disease.

Complete blood counts were determined by automated procedures for all subjects included in the study. There were no statistically significant differences between IgAN patients and HS for all parameters considered (Supplementary Table S6). Furthermore, as described by other investigators, the composition of the major immunological subsets in IgAN is similar between patients and controls.<sup>14</sup>

For microarray analysis and RT-PCR validation, we randomly selected 12 IgAN patients' and 8 HS samples. In all, 16 IgAN patients' and 16 HS samples were used to evaluate the pathways emerging from microarray analysis using classical biomolecular approaches on PBMCs. For this purpose, we randomly selected subgroups of IgAN patients and HS, as the biological material obtained from each subject was not sufficient to perform all the functional genomic studies in triplicate. The remaining blood samples obtained from 10 IgAN patients and 10 HS were used for the studies on PBMC subpopulations. Three membranoproliferative glomerulonephritis type I and three focal segmental glomerulosclerosis patients were used for the GSEA. Those having the same demographic and clinical features as that of IgAN patients were selected as disease controls.

The study was carried out according to the principles of the Declaration of Helsinki and was approved by our institutional ethics review board.

### Sample processing and microarray hybridization

As gene expression profiles of whole blood cells are normally highly sensitive for *ex vivo* incubation,<sup>48</sup> samples used for microarray were collected with PAXgene Blood RNA System (PreAnalytiX, Heidelberg, Germany), in which the RNA-stabilizing reagents in the collection tube ensure that transcription profiles reflect the actual physiological state at the time of the blood drawn.<sup>49</sup> RNA was extracted immediately using a PaxGene blood RNA isolation kit (Qiagen, Valencia, CA, USA). RNA (5  $\mu$ g) was treated using the Globin Reduction Protocol according to the manufacturer's directions (Affymetrix, Santa Clara, CA, USA), and was checked by electrophoresis using the Agilent 2100 bioanalyzer (Agilent, Palo Alto, CA, USA). It was then processed and hybridized to the GeneChip Human Genome U133A oligonucleotide microarray (Affymetrix) containing 22,283 gene probe sets, representing 12,357 well-characterized human genes and 3800 expressed sequence tags. Scaled gene expression values were calculated and normalized using the default setting of Affymetrix Microarray Suite (MAS) software version 5.0. The data discussed in this publication have been deposited in NCBI's Gene Expression Omnibus (GEO, <http://www.ncbi.nlm.nih.gov/geo/>) and are accessible through GEO Series accession number GSE14795.

### Quantitative RT-PCR analysis

Total RNA (1  $\mu$ g) isolated from 12 IgAN patients and 8 HS was reverse transcribed with High-Capacity cDNA Reverse Transcription (Applied Biosystems, Foster City, CA, USA) according to the manufacturer's instructions. Quantitative RT-PCR amplification reactions were performed in triplicate in 25  $\mu$ l final volumes using SYBR Green chemistry on an iCycler (Bio-Rad Laboratories, Hercules, CA, USA) for *INV* and *PTEN*. Quantitative RT-PCR was performed using the QuantiTect Primer Assay (Qiagen, Basel,

Switzerland) and the QuantiFast SYBR Green PCR mix (Qiagen). Genes were amplified according to the manufacturer's directions. The  $\beta$ -actin gene amplification was used as a reference standard to normalize the target signal. For PCR array, cDNA from 500  $\mu$ g total RNA extracted with RNeasy Mini kit (Qiagen) was synthesized using RT<sup>2</sup> first strand kit (SABiosciences Corporation). PCR array (Human WNT signaling Pathway RT<sup>2</sup>Profiler PCR Array, SABiosciences Corporation) was performed according to manufacturer's instructions and using three biological replicates for each of the three subpopulations isolated from four IgAN patients and four HS subjects.

### **PBMC, monocyte, B-, and T-lymphocyte subpopulation isolation and protein extraction**

Peripheral blood mononuclear cells were isolated by density gradient centrifugation. Monocytes, B-, and T-lymphocytes were obtained from PBMCs by immunolabelling the sample sequentially with positive selection kits according to the manufacturer's specifications (EasySep, StemCell Technologies, Vancouver, Canada); the obtained preparations were typically >95% CD3<sup>+</sup> CD19<sup>+</sup> CD14<sup>+</sup> by flow cytometric analysis (data not shown). Cells were then counted and their viability was determined by trypan blue staining. Isolated cells were lysed in RIPA buffer on ice for 30 min and centrifuged at 10,000 g at 4 °C for 10 min. The supernatants, containing total proteins, were collected and stored at -80 °C. Total protein concentration was determined with the standard Bradford colorimetric assay (Bio-Rad Laboratories, Richmond, CA, USA).

### **Western blot analysis for INV**

Aliquots containing 100  $\mu$ g of proteins from each lysate were subjected to sodium dodecyl sulfate polyacrylamide gel electrophoresis on a 7.5% gel under reducing conditions and then electrotransferred onto PVDF membrane (HybondTM, Amersham, UK). Membranes were probed with primary antibody to INV (mouse anti-INV antibody, 1:500; Abnova, Taipei, Taiwan) and incubated with secondary antibody (horseradish peroxidase-conjugated goat anti-mouse 1:20,000; Bio-Rad Laboratories). Horseradish peroxidase was detected with LiteAblot (Euroclone, Milan, Italy) and chemiluminescence was detected on ECL films (Eastman Kodak, Rochester, NY, USA). The same membranes were stripped and proteins were rehybridized with anti- $\beta$ -actin antibody (1:10,000; Sigma, Milan, Italy, A1978). Images were acquired using a scanner EPSON Perfection 2580 Photo (EPSON, Long Beach, CA, USA) and quantified by Image J 1.34 Software (<http://rsb.info.nih.gov/ij/>). The intensity of bands, corresponding to the INV protein, was normalized to the actin signal.

### **ELISA for Akt and PTEN**

For the Akt measurement, an enzyme-linked immunosorbent assay (ELISA) kit specific for P-Ser473 Akt was used, according to the manufacturer's protocol, and the results were normalized to the total Akt content (Akt (total) ELISA kit and Akt (pS473) ELISA kit; Bio-Ssource, Camarillo, CA, USA). For PTEN, we used a specific Duo-Set, ELISA development system (R&D Systems, Europe, Abingdon, UK), according to the manufacturer's instructions. Data generated were then normalized to total protein content.

### **Nuclear $\beta$ -catenin determination**

Cytoplasmic and nuclear extracts were obtained with NE-PER lysis buffers according to the supplier's instructions (NE-PER, Perbio, Bonn, Germany). To evaluate  $\beta$ -catenin concentration in cytoplasmic and nuclear extracts, the TiterZyme immunometric assay (EIA)

for  $\beta$ -catenin (Assay Designs, Ann Arbor, MI, USA) was used. Both cytoplasmic and nuclear values of  $\beta$ -catenin were normalized to the respective total protein concentration. The translocation rate was then calculated using the ratio between normalized nuclear  $\beta$ -catenin and normalized cytoplasmic  $\beta$ -catenin.

### **PBMC proliferation test**

Isolated PBMCs were plated, at  $1 \times 10^5$  cells per well, in flat-bottomed 96-well plates (Costar Corning, Corning, NY, USA) in complete culture medium (RPMI-1640 supplemented with antibiotics, 2 mM L-glutamine, 1 mM sodium pyruvate, 1 mM nonessential amino acids 0.05 mM 2-mercapto-ethanol, 25 mM HEPES (4-(2-hydroxyethyl)-1-piperazineethanesulfonic acid) buffer, and 10% fetal bovine serum) and cultured for 5 days at 37 °C in 5% CO<sub>2</sub>. Experiments were performed in quadruplicate, that is, four test wells with mitogenic stimulation added at a final concentration of 5  $\mu$ g/ml of concanavalin A (Sigma, C5275), 0.075% (wt/vol) of *Staphylococcus aureus* Cowan (Pansorbin, Calbiochem), and 10  $\mu$ g/ml of pokeweed mitogen (Sigma, L8777), and four control wells without stimulation. Cell proliferation was measured by a colorimetric immunoassay evaluating incorporated nuclear BrdU (5-bromo-2-deoxyuridine), according to the manufacturer guidelines (Roche Diagnostics GmbH, Mannheim, Germany). All experiments for each subject were performed four times, proliferation was expressed as a proliferation index  $\pm$  s.e.m., calculated as the ratio between the BrdU absorbance in the test and that in the control wells.

### **Statistical analysis and bioinformatics**

For microarray analysis, the raw expression signals were log-transformed and filtered-out, if assigned by MAS 5.0 as 'absent' in all samples in the cohort, which resulted in the selection of 15,450 probes out of the original 22,283 set. The preprocessed microarray data were imported into the R language for statistical analysis computing (<http://www.r-project.org>). Genes displaying differential expression between IgAN patients and HS were detected using a two-sample *t*-test. Gene probe sets were sorted after significant *P*-value and were adjusted to account for multiple testing using the FDR method of Storey and Tibshirani.<sup>50</sup> Only genes that were significantly (FDR-adjusted; *P*-value < 0.005) modulated in IgAN patients compared with HS, were considered for further analysis. Two-dimensional hierarchical clustering was performed using Spotfire decision site 8.0 (<http://spotfire.tibco.com>). GSEA<sup>21</sup> was performed using GeneSpring GX 9.0 (Agilent Technologies Inc., Palo Alto, CA, USA). For this analysis, a gene set was created starting from genes discriminating IgAN patients from HS, considering for each gene a fold change value >2. Significance of differential expression, as determined by the enrichment analysis, was recalculated 1000 times. A corrected *P*-value was obtained from the analysis using the FDR *q*-value correction. On the basis of this correction, the cutoff for significance was established at a *P*-value  $\leq$  0.05. The PCR array analysis was carried out using the manufacturer's data analysis tool (<http://www.sabiosciences.com/pcr/arrayanalysis.php>). To assess biological relationships among genes, we used the Ingenuity Pathway Analysis software (IPA, Ingenuity System, Redwood City, CA, USA; <http://www.ingenuity.com>). IPA computes a score for each network according to the fit of the set of supplied focus genes (here, genes differently expressed in IgAN patients). These scores indicate the likelihood of focus genes to belong to a network versus those obtained by chance. A score >2 indicates a  $\leq$  99% confidence that a focus gene network was not generated by chance alone. The canonical pathways generated by IPA

are the most significant for the uploaded data set. Fischer's exact test with FDR option was used to calculate the significance of the canonical pathway.

All values were expressed as the mean  $\pm$  s.e.m. of data obtained from at least three independent experiments. Two-tailed Student's *t*-test was used to assess differences in biological features among IgAN patients and HS. Pearson's correlation test was used to study continuous variables.

#### DISCLOSURE

All the authors declared no competing interests.

#### ACKNOWLEDGMENTS

We are grateful to the patients for their cooperation in this study. We are grateful to M Carella for microarray hybridization. We also thank S Volinia and S Rossi for the technical assistance in microarray statistical analysis. This work was supported by grants from the MiUR (COFIN-PRIN 2006069815) and FIRB (RBNE013JYM).

#### SUPPLEMENTARY MATERIAL

**Table S1.** Downregulated genes in IgAN patients.

**Table S2.** Upregulated genes in IgAN patients.

**Table S3.** Deregulated WNT pathway genes in monocytes isolated from IgAN patients.

**Table S4.** Deregulated WNT pathway genes in B-lymphocytes isolated from IgAN patients.

**Table S5.** Deregulated WNT pathway genes in T-lymphocytes isolated from IgAN patients.

**Table S6.** Complete blood counts of the study population (IgAN patients and healthy subjects).

**Figure S1.** Gene set enrichment analysis.

**Figure S2.** Total Akt in IgAN patients and healthy subjects.

Supplementary material is linked to the online version of the paper at <http://www.nature.com/ki>

#### REFERENCES

- Radford MG, Donadio Jr JV, Bergstrahl Jr EJ *et al.* Predicting renal outcome in IgA nephropathy. *J Am Soc Nephrol* 1997; **8**: 199–207.
- D'Amico G. Natural history of idiopathic IgA nephropathy: role of clinical and histological prognostic factors. *Am J Kidney Dis* 2000; **36**: 227–237.
- Allen AC, Bailey EM, Brenchley PE *et al.* Mesangial IgA1 in IgA nephropathy exhibits aberrant O-glycosylation: observations in three patients. *Kidney Int* 2001; **60**: 969–973.
- Novak J, Tomana M, Matousovic K *et al.* IgA1-containing immune complexes in IgA nephropathy differentially affect proliferation of mesangial cells. *Kidney Int* 2005; **67**: 504–513.
- Manno C, Torres DD, Rossini M *et al.* Randomized controlled clinical trial of corticosteroids plus ACE-inhibitors with long-term follow-up in proteinuric IgA nephropathy. *Nephrol Dial Transplant* 2009; **24**: 3694–3701.
- Van der Boog PJ, de Fijter JW, Bruijn JA *et al.* Recurrence of IgA nephropathy after renal transplantation. *Ann Med Interne* 1999; **150**: 137–142.
- Ponticelli C, Traversi L, Feliciani A *et al.* Kidney transplantation in patients with IgA mesangial glomerulonephritis. *Kidney Int* 2001; **60**: 1948–1954.
- Koselj M, Rott T, Kandus A *et al.* Donor-transmitted IgA nephropathy: long-term follow-up of kidney donors and recipients. *Transplant Proc* 1997; **29**: 3406–3407.
- Sanfilippo F, Croker BP, Bollinger RR. Fate of four cadaveric donor renal allografts with mesangial IgA deposits. *Transplantation* 1982; **33**: 370–376.
- Fortune F, Courteau M, Williams DG *et al.* T and B cell responses following immunization with tetanus toxoid in IgA nephropathy. *Clin Exp Immunol* 1992; **88**: 62–67.
- van den Wall Bake AW, Beyer WE, Evers-Schouten JH *et al.* Humoral immune response to influenza vaccination in patients with primary immunoglobulin A nephropathy. An analysis of isotype distribution and size of the influenza-specific antibodies. *J Clin Invest* 1989; **84**: 1070–1075.
- Barratt J, Bailey EM, Buck KS *et al.* Exaggerated systemic antibody response to mucosal *Helicobacter pylori* infection in IgA nephropathy. *Am J Kidney Dis* 1999; **33**: 1049–1057.
- Kennel-de March A, Bene MC, Renoult E *et al.* Enhanced expression of L-selectin on peripheral blood lymphocytes from patients with IgA nephropathy. *Clin Exp Immunol* 1999; **115**: 542–546.
- Batra A, Smith AC, Feehally J *et al.* T-cell homing receptor expression in IgA nephropathy. *Nephrol Dial Transplant* 2007; **22**: 2540–2548.
- Harper SJ, Allen AC, Béné MC *et al.* Increased dimeric IgA-producing B cells in tonsils in IgA nephropathy determined by *in situ* hybridization for J chain mRNA. *Clin Exp Immunol* 1995; **101**: 442–448.
- Harper SJ, Allen AC, Pringle JH *et al.* Increased dimeric IgA producing B cells in the bone marrow in IgA nephropathy determined by *in situ* hybridisation for J chain mRNA. *J Clin Pathol* 1996; **49**: 38–42.
- Kodama S, Suzuki M, Arita M *et al.* Increase in tonsillar germinal centre B-1 cell numbers in IgA nephropathy (IgAN) patients and reduced susceptibility to Fas-mediated apoptosis. *Clin Exp Immunol* 2001; **123**: 301–308.
- Lai AS, Lai KN. Molecular basis of IgA nephropathy. *Curr Mol Med* 2005; **5**: 475–487.
- Preston GA, Waga I, Alcorta DA *et al.* Gene expression profiles of circulating leukocytes correlate with renal disease activity in IgA nephropathy. *Kidney Int* 2004; **65**: 420–430.
- Simons M, Gloy J, Ganner A *et al.* Inversin, the gene product mutated in nephronophthisis type II, functions as a molecular switch between WNT signaling pathways. *Nat Genet* 2005; **37**: 537–543.
- Subramanian A, Tamayo P, Mootha VK *et al.* Gene set enrichment analysis: a knowledge-based approach for interpreting genome-wide expression profiles. *Proc Natl Acad Sci USA* 2005; **102**: 15545–15550.
- Iwata Y, Wada T, Uchiyama A *et al.* Remission of IgA nephropathy after allogeneic peripheral blood stem cell transplantation followed by immunosuppression for acute lymphocytic leukemia. *Intern Med* 2006; **45**: 1291–1295.
- Sakai H. Cellular immunoregulatory aspects of IgA nephropathy. *Am J Kidney Dis* 1988; **12**: 430–432.
- Coppo R, Camilla R, Alfarano A *et al.* Upregulation of the immunoproteasome in peripheral blood mononuclear cells of patients with IgA nephropathy. *Kidney Int* 2009; **75**: 536–541.
- Sakai A, Thieblemont C, Wellmann A *et al.* PTEN gene alterations in lymphoid neoplasms. *Blood* 1998; **92**: 3410–3415.
- Shan X, Czar MJ, Bunnell SC *et al.* Deficiency of PTEN in Jurkat T cells causes constitutive localization of Itk to the plasma membrane and hyperresponsiveness to CD3 stimulation. *Mol Cell Biol* 2000; **20**: 6945–6957.
- Monick MM, Carter AB, Robeff PK *et al.* Lipopolysaccharide activates Akt in human alveolar macrophages resulting in nuclear accumulation and transcriptional activity of beta-catenin. *J Immunol* 2001; **166**: 4713–4720.
- Lawlor MA, Alessi DR. PKB/Akt: a key mediator of cell proliferation, survival and insulin responses? *J Cell Sci* 2001; **114**: 2903–2910.
- Masckauchán TN, Shawber CJ, Funahashi Y *et al.* Wnt/ $\beta$ -catenin signalling induces proliferation, survival and IL-8 in human endothelial cells. *Angiogenesis* 2005; **8**: 43–51.
- Barratt J, Feehally J. IgA nephropathy. *J Am Soc Nephrol* 2005; **16**: 2088–2097.
- Di Cristofano A, Kotsi P, Peng YF *et al.* Impaired Fas response and autoimmunity in Pten<sup>+/-</sup> mice. *Science* 1999; **285**: 2122–2125.
- Suzuki A, Kaisho T, Ohishi M *et al.* Critical roles of Pten in B cell homeostasis and immunoglobulin class switch recombination. *J Exp Med* 2003; **197**: 657–667.
- Parsons MJ, Jones RG, Tsao MS *et al.* Expression of active protein kinase B in T cells perturbs both T and B cell homeostasis and promotes inflammation. *J Immunol* 2001; **167**: 42–48.
- Reya TM, O'Riordan R, Okamura E *et al.* Wnt signaling regulates B lymphocyte proliferation through a LEF-1 dependent mechanism. *Immunity* 2000; **13**: 15–24.
- Bisceglia L, Cerullo G, Forabosco P *et al.* Genetic heterogeneity in Italian families with IgA nephropathy: suggestive linkage for two novel IgA nephropathy loci. *Am J Hum Genet* 2006; **79**: 1130–1134.
- Mikels AJ, Nusse R. WNTs as ligands: processing, secretion and reception. *Oncogene* 2006; **25**: 7461–7468.
- Lee YN, Gao Y, Wang HY. Differential mediation of the Wnt canonical pathway by mammalian dishevelleds-1, -2, and -3. *Cell Signal* 2008; **20**: 443–452.
- Gordon MD, Nusse R. WNT signaling: multiple pathways, multiple receptors, and multiple transcription factors. *J Biol Chem* 2006; **281**: 22429–22433.
- Xie H, Huang Z, Sadim MS *et al.* Stabilized  $\beta$ -catenin extends thymocyte survival by up-regulating Bcl-xL. *J Immunol* 2005; **175**: 7981–7988.

40. Staal FJ, Luis TC, Tiemessen MM. WNT signalling in the immune system: WNT is spreading its wings. *Nat Rev Immunol* 2008; **8**: 581–593.
41. Thiele A, Wasner M, Muller C *et al*. Regulation and possible function of beta-catenin in human monocytes. *J Immunol* 2001; **167**: 6786–6793.
42. George SJ. Wnt pathway: a new role in regulation of inflammation. *Arterioscler Thromb Vasc Biol* 2008; **28**: 400–402.
43. Blumenthal A, Ehlers S, Lauber J *et al*. The Wingless homolog WNT5A and its receptor Frizzled-5 regulate inflammatory responses of human mononuclear cells induced by microbial stimulation. *Blood* 2006; **108**: 965–973.
44. Monteiro RC, Moura IC, Launay P *et al*. Pathogenic significance of IgA receptor interactions in IgA nephropathy. *Trends Mol Med* 2002; **8**: 464–468.
45. Launay P, Grossetete B, Arcos-Fajardo M *et al*. Fc $\alpha$  receptor (CD89) mediates the development of immunoglobulin A (IgA) nephropathy (Berger's disease): evidence for pathogenic soluble receptor-IgA complexes in patients and CD89 transgenic mice. *J Exp Med* 2000; **191**: 1999–2009.
46. Wines BD, Hulett MD, Jamieson GP *et al*. Identification of residues in the first domain of human Fc $\alpha$  receptor essential for interaction with IgA. *J Immunol* 1999; **162**: 2146–2153.
47. Bracke M, Nijhuis E, Lammers JW *et al*. A critical role for PI3-kinase in cytokine-induced Fc $\alpha$ -receptor activation. *Blood* 2000; **95**: 2037–2043.
48. Baechler EC, Batliwalla FM, Karypis G *et al*. Expression levels for many genes in human peripheral blood cells are highly sensitive to *ex vivo* incubation. *Genes Immun* 2004; **5**: 347–353.
49. Rainen L, Oelmueller U, Jurgensen S *et al*. Stabilization of mRNA expression in whole blood samples. *Clin Chem* 2002; **48**: 1883–1890.
50. Storey JD, Tibshirani R. Statistical significance for genome wide studies. *Proc Natl Acad Sci USA* 2003; **100**: 9440–9445.